Proceedings of the 8th U.S. National Conference on Earthquake Engineering
April 18-22, 2006, San Francisco, California, USA
Paper No. 1177

CONFINING MASONRY USING PRE-CAST RC ELEMENT FOR ENHANCED EARTHQUAKE RESISTANCE

Samaresh Paikara[1] and Durgesh C. Rai[2]

ABSTRACT

Un-reinforced Masonry (URM) buildings which are designed and constructed only for gravity forces and not for lateral forces, present challenging engineering problems in seismic disaster mitigation. Some conventional designs of URM structures have shown acceptable performance during past earthquakes. Earthquake resistance of these structures depends on energy dissipation potential of well-detailed portions such that it can undergo large but controlled inelastic deformations in the event of design earthquakes. In such URM walls, a grid of horizontal, vertical and/or diagonal elements, break a large wall into smaller wall areas and confine them. These structures respond to the stress of the earthquake by working along the joints between infill and confinement elements; the straining and sliding of masonry and confining elements dissipates a significant amount of energy during earthquake. The primary thrust of this paper is to investigate the seismic behaviour of such confinement schemes on URM using RC pre-cast grid elements. Both analytical and experimental work on behaviour of confinement schemes is presented. The analytical work has been carried out by Finite Element Model using ABAQUS, whereas, the experimental work is based on pseudo-static cyclic tests on half-scale wall specimens.

Introduction

In the recent earthquakes of Kashmir (2005), Bam (2003), Bhuj (2001) and Turkey (1999), which observed high death toll, damages and collapse occurred to contemporary non-engineered buildings rather than traditional ones. These earthquakes have vividly demonstrated seismic vulnerability of a large number of masonry buildings, particularly the existing Unreinforced Masonry (URM) buildings. Such URM buildings designed only for gravity forces and not for lateral forces, represent challenging engineering problems in disaster mitigation.

Post-earthquake reconnaissance have pointed out that diagonal shear cracking through the weaker masonry units was predominant mode of failure and there was less or no chance of sliding at the interface of the masonry units or panel walls. On the contrary, conventional earthquake resistant design of structures relies on energy dissipation potential of well detailed portions and/or members of structures which undergo large but controlled inelastic deformations

[1]Former Graduate Student, Department of Civil Engineering, Indian Institute of Technology Kanpur, Kanpur 208016, India. Email: spaikara@gmail.com
[2]Assistant Professor, Department of Civil Engineering, Indian Institute of Technology Kanpur, Kanpur 208 016, India. Email: dcrai@iitk.ac.in

during earthquakes. Cracking in masonry is not inconsistent with the conventional earthquake resistant design philosophy, however, it must be controlled in such a way that the cracked masonry does not seriously undermine the vertical load carrying capacity of the URM wall. Confining masonry in small panels by grid elements distributes cracking (inelastic activities) through out the URM wall. The grid of horizontal, vertical and/or diagonal elements break a large wall into smaller wall areas panels which are adequately confined by surrounding grid elements at the boundaries.

Timber lacing the masonry walls is a traditional method of masonry construction for earthquake-resistance, such as those found in Kashmir, India in the form of *Dhajji-dewari* or *Taq* system of masonry wall construction. The basic features of this timber-laced masonry construction are (a) the use of horizontal timbers embedded into bearing wall masonry, and (b) the insertion of masonry in between columns, beams and studs of a complete timber frame. Presence of timber studs, which subdivides the infill, arrests the loss of the portion or all of several masonry panels and resisted progressive destruction of the rest of the wall. The closely spaced studs prevent propagation of diagonal shear cracks within any single panel, and reduce the possibility of the out-of-plane failure of masonry (Gülkan and Langenbach 2004) (Figure 1).

(a) (b)

Figure 1 Traditional masonry for proven earthquake resistance: (a) *Dhajji-dewari* system of timber laced masonry for confining masonry in small panels and (b) *Taq* system of embedding timber thick walls

Experimental Investigation of the Confined Masonry Walls

An experimental work has been carried out on half scale models of confined wall specimens of dimensions 2.5 m × 1.5 m with two different configurations of confinement schemes: (a) Confinement scheme 1 consisted of boundary and one vertical confining element, which divided the whole wall into two panels, as shown in Figure 2a, and (b) Confinement scheme 2 consisted of boundary, one vertical, two horizontal and two diagonal confining elements, which divided the whole wall into eight panels, as shown in Figure 2b (Paikara 2005).

The cross-sections of the confining grid elements were 60 mm × 40 mm (Width × Thickness). Two reinforcing wires were provided in the middle of the cross section of the confining grid elements. In the first model all confining grid elements were 40 mm deep. However, in the second specimen, the depth of top horizontal confining grid elements were increased to 100 mm

for better grip of load transferring mechanism from actuator. Confining grid elements of the specimens were cast in wooden mould separately and were demolded after 24 hours and moist cured for 28 days. After curing they were assembled in a grid by connecting them with the help of 90º bend metal straps of 3 mm × 25 mm cross-section having legs of 150 mm. The metal straps were secured in place by 6 mm diameter bolts through holes in grid elements left in the concrete sections at proper places during casting.

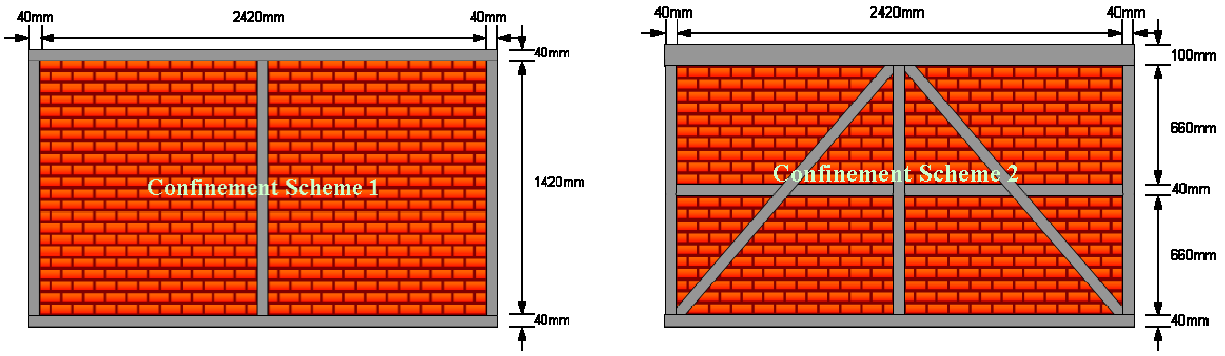

(a) (b)

Figure 2 (a) Confinement scheme 1, (b) Confinement scheme 2 used in experimental studies

The wall panels were half-brick thick and made with lime cement mortar of 1:1:6 (cement: lime: sand) proportion by weight. Masonry was constructed inside the panels. Well-burnt specially manufactured 1:2 scaled model bricks were used in the test specimens. The average dimensions of the bricks were 120:59.6:34 mm. The masonry walls were left un-plastered and moist cured by regularly sprinkling water on the surface.

Slow cyclic tests were performed on confined masonry specimens. The specimens were connected to the bottom beam, which was connected to the floor by proper fasteners. The load from the actuator was transferred to the top confining grid element, which is almost analogous to the application of load at the floor level of prototype structure. An arrangement was made with four tie rods to pull the specimens in negative loading direction (Figure 3).

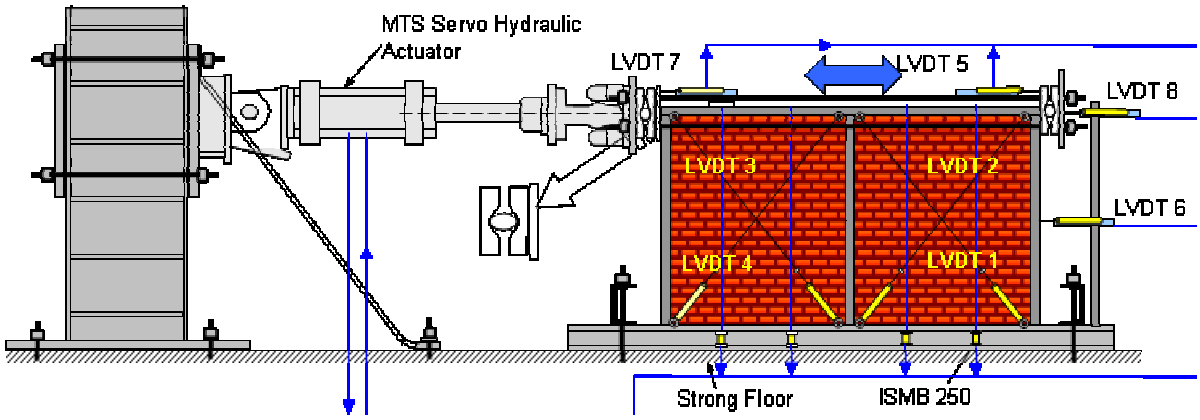

Figure 3 Block diagram of the testing system used in the present experimental study

No vertical load was applied in model with confinement scheme 1, however, in case of confinement scheme 3, vertical load of 15 kN by means of post-tensioned cables was applied to

maintain a vertical pressure of 0.1 MPa on the specimen. Displacements at different locations of the topmost horizontal confining grid element and two main panels were measured using LVDTs. LVDTs measured the diagonal displacement in the two main panels of the confined wall, in addition to horizontal displacement in the topmost horizontal confining grid element.

Observations from the Tests

Confinement Scheme 1

The first crack formed at the interface of masonry and vertical grid element at a displacement excursion level of +2 mm when vertical separation cracks formed at both ends of vertical interfaces. These vertical separation cracks intensified with increase in displacement excursion and slightly inclined cracks started to form at the corner regions of panels at displacement excursion level of +3 mm. Flexural cracks in the vertical grid elements were observed at a displacement excursion level of +4 mm. Diagonal stepped cracks started to form from the edge at +5 mm displacement and those cracks reached mid-length at 12 mm displacement excursion level. The ultimate load of 22.5 kN was observed at a displacement of +6 mm. Some amount of corner crushing was observed at 8 mm displacement excursion level. At 15 mm displacement cycle crack width increased upto 10 mm. Snapping of one vertical member was observed at displacement excursion level of 25 mm. However, the displacement cycle of 30 mm was continued and during this the specimen resisted about 75% of the ultimate load. The specimen at the end of the test is shown in Figure 4a.

(a) (b)

Figure 4 (a) Specimen 1 and (b) Specimen 2 at the conclusion of the test

Confinement Scheme 2

In the second specimen the first crack formed at the interface of diagonal grid elements and end masonry panels at a displacement excursion level of +3 mm. The next prominent cracking was visible at a displacement excursion level of 5 mm at top trapezoidal panel in the loading side which were diagonal cracks through the mortar joints which intensified further with increase in displacement excursion. At displacement excursion level of +6 mm slightly inclined cracks started to form at the corner regions of panels. Horizontal cracks started to form from the edge at +8 mm displacement and those cracks reached the diagonal grid at 12 mm displacement excursion level. In 15 mm displacement excursion level, horizontal cracks began to form at the lower trapezoidal panels also. The ultimate load of 53.4 kN was observed at a displacement of

+20 mm. During the 20 mm displacement cycle almost all the interfaces of the grid elements and masonry separated and opening and closing of cracks were observed. At 30 mm displacement excursion level, horizontal cracks were observed at bottom trapezoidal panel opposite to the loading side. Bending of one vertical member was observed at displacement excursion level of 35 mm and flexural cracks were observed. At the displacement cycle of 40 mm, a 50% reduction from the ultimate strength was noted, however, there was no sign of corner crushing and horizontal and diagonal cracks through the mortar at different places of the panels, which signifies the shear mode of failure. The failed specimen is shown in Figure 4b.

Load Displacement Response

The lateral load displacement hysteretic response for specimens 1 and 2 is shown in Figure 5. The envelope backbone curves of the specimens are shown in Figure 6. Specimen 1 reached its ultimate load 22.5 kN at a displacement level of 6 mm, whereas specimen 2 reached its ultimate load of 53.4 kN at 20 mm cycle. For specimen 2 the higher load carrying capacity and higher displacement level to reach the ultimate load can be contributed to better confinement and introduction of preferred plane of slippage and the sliding mode of failure. The initial stiffness of specimens 1 and 2 were found to be 11.4 kN/mm and 14.0 kN/mm, respectively.

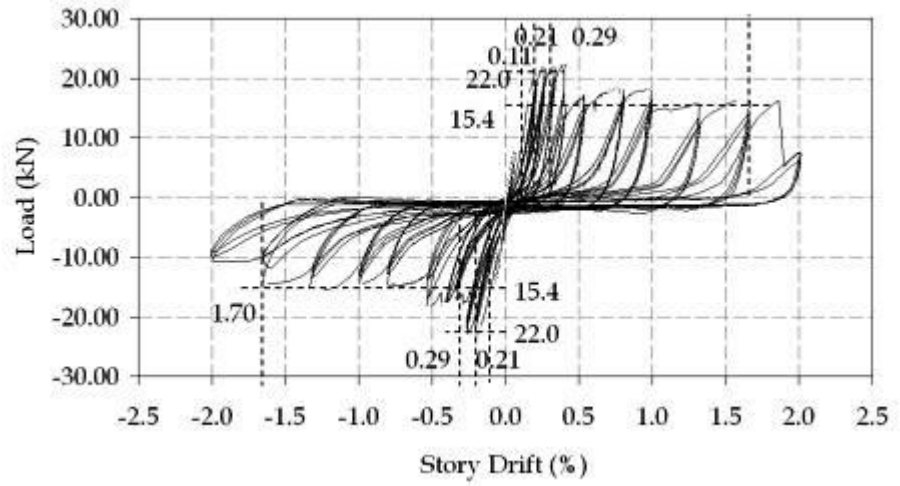

(a)

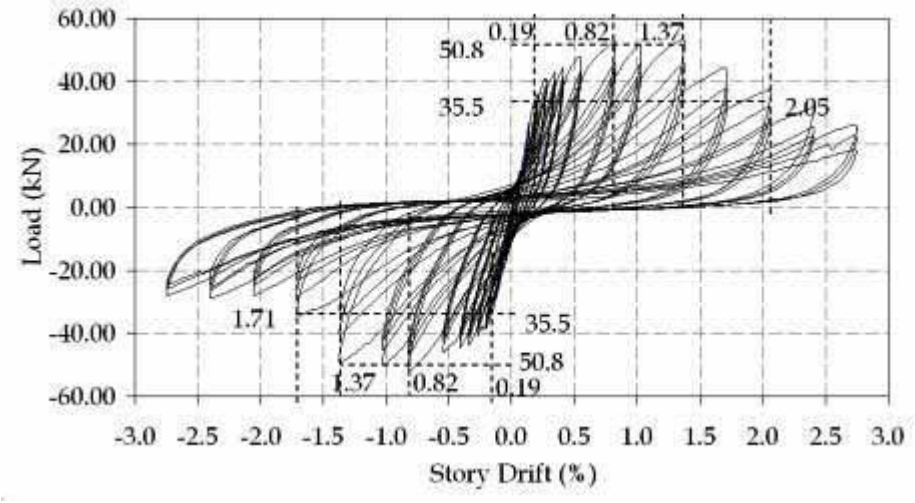

(b)

Figure 5 Load-deformation behaviour of (a) Specimen 1and (b) Specimen 2

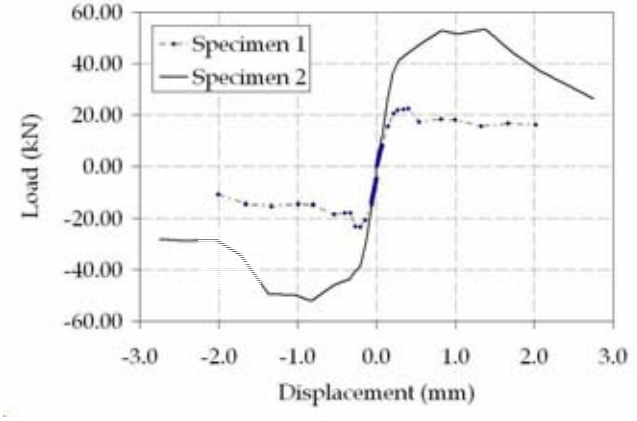

Figure 6 Envelope values of shear resistance of the specimens

Cycle Stiffness

As observed in the hysteretic response of all the specimens, the lateral stiffness of the specimens and panels was on continuous decline with each cycle of increasing displacement. This stiffness degradation between different loading sequences can be indicated as a change in the slope of the line joining the maximum excursion point in the positive cycle and the maximum excursion point in the negative cycle, also referred as cyclic stiffness. As shown in Figure 7, the stiffness of the Specimen 2 improved with introduction of more grid elements at all story drift levels.

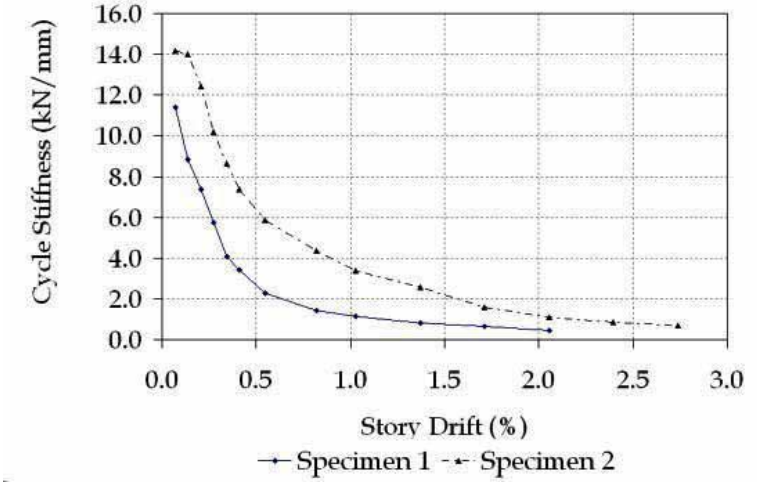

Figure 7 Variation of the cycle stiffness of specimens with story drift.

Energy Dissipated

The energy dissipated in each cycle is the area enclosed by the hysteresis loop corresponding to that cycle. The energy dissipated by whole wall corresponds to total wall force and the horizontal displacement of the wall. The energy dissipated per unit volume by panels is calculated from the average stress and strain in the panels. The average stress is calculated by dividing the applied force by the cross-sectional area of the wall. The strain is calculated from the displacement measured by the diagonal LVDTs on the panels. Comparative plots of cumulative energy dissipated per unit volume vs. cumulative strain and cumulative energy dissipated per unit

volume vs. story drift of different specimens are shown in Figure 8a and 8b.

Plots of total cumulative energy dissipated vs. story drift for two specimens and their two main panels are shown in Figure 8c and 8d. The results show that for specimen 1 and specimen 2 the energy dissipation per unit volume is the almost same for panels and whole wall. From the plots, it is found that sum of energy dissipated by the panels almost matched with the energy dissipated by the whole wall in case of specimen 1 and specimen 2. However, for specimen 2, sum of energy dissipated by the two main panels were somewhat lesser than the energy dissipated by the whole wall.

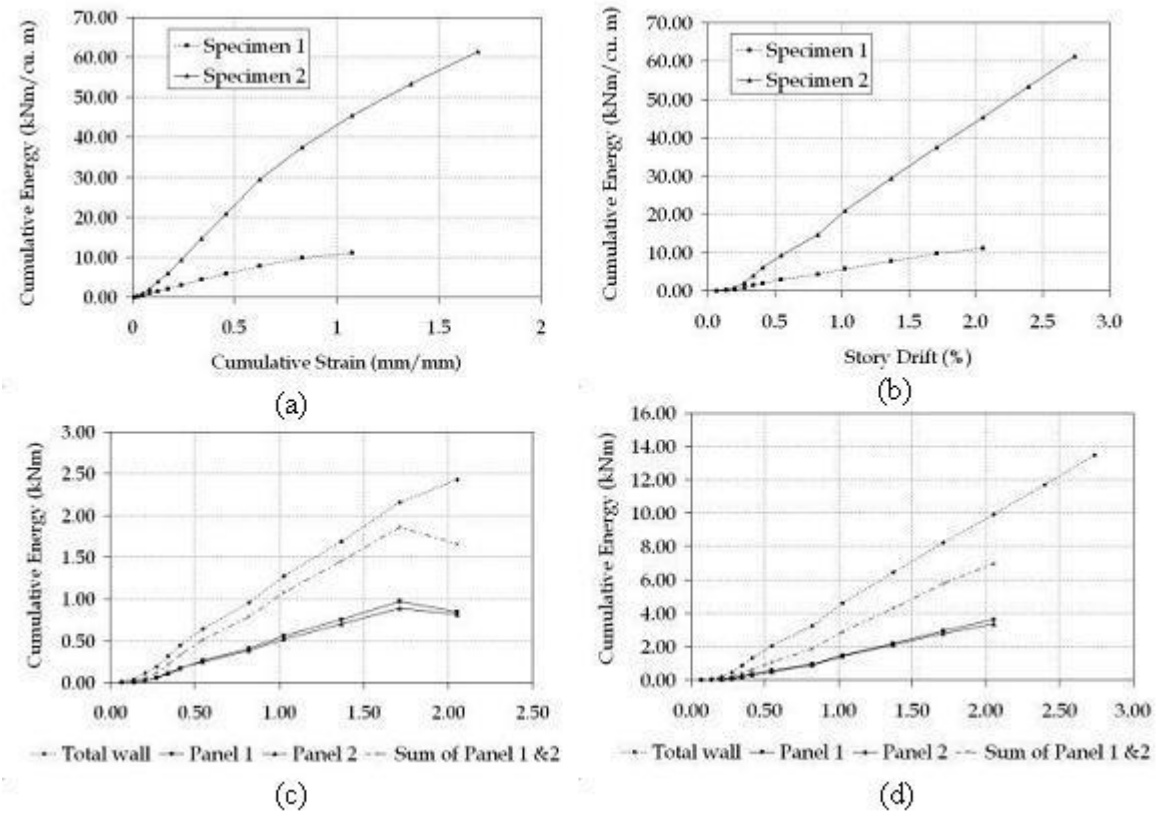

Figure 8 (a) Cumulative energy dissipated per unit volume vs. cumulative strain (b) Cumulative energy dissipated per unit volume vs. story drift (c) Cumulative energy dissipated vs. story drift in specimen 1 (d) in specimen 2

Analytical Investigation of the Confined Masonry Walls

ABAQUS was used for FE analyses in which masonry was modelled at macroscopic level. However, the interaction between the different constituents of the confinement system and the interaction between the masonry and its confinement was done in microscopic level. The test specimens were differentiated into a mixture of different finite elements. A two dimensional continuum in the state of plane stress was considered for the masonry portion. Two-dimensional linear elements were used to model the grid elements of the confinement schemes. The discretization of masonry was done by 0.05 m square sized, 4-noded iso-parametric CPS4R type elements of ABAQUS element library. Standard beam element of type B21 was used to model

the confining grid elements.

Inhibitory computational cost and complexities involved with FE analysis for cyclic loading restricted the study to only monotonic loading. However, this curtailed scheme of analysis is capable of providing essential load deformation behaviour of the confined masonry walls. The model is incapable of handling the strength and stiffness degradation associated with reverse cyclic loading, which is associated with typical earthquake type motion.

Material Modelling

The material behaviour of the masonry was modelled with the material option *CONCRETE. Material option *CONCRETE covers most of the characteristics of a brittle material in terms of its non-linear stress-strain relationship, cracking and failure (Rai & Goel 1996, Chuang et al. 2004). The properties used are obtained mostly from the experimentally observed results. Young's modulus for the masonry used in the experimental models was found to be 1388 MPa by masonry prism tests. The value of Poisson's ratio taken for all the masonry was 0.2. For steel reinforcement used in concrete confining grid members Young's modulus and Poisson's ratio were taken as 210 GPa and 0.3, respectively. For fibre reinforced concrete Young's modulus was measured 55 GPa and Poisson's ratio was taken as 0.15, respectively. For other properties that could not be experimentally obtained, results reported in the literature were used (Rai & Goel 1996, Buonopane et al. 1999, Magenes and Calvi 2002).

Boundary Condition and Loading

The appropriate boundary conditions were achieved by either deleting or constraining relevant nodal degrees of freedom of various elements. All the degrees of freedom of the nodes in bottom most elements were deleted in order to simulate a fixed boundary condition. Connections between confining elements were modelled as hinge joint with rotational springs to specify their moment-rotation behaviour. However, the translational movement between the different confining grid elements was restricted. This simplification will have little effect on the load deformation relation. The main concept behind the new confinement scheme is presence of high energy dissipating capacity due to friction at the interface of the masonry and confining grid elements. Appropriate description of the interface between the confining grid elements and masonry modelled the frictional behaviour at the interface. However, due to complicacy in the interface modelling between the each masonry unit and mortar each masonry panel was modelled as a single unit. This simplification will not act upon the behaviour of the system as a whole, as the modelling of a masonry panel as a single part is capable of taking care of the cracks and deformation in the masonry.

Regarding the loading, the models were subjected to a constant vertical loading to represent the loads from the upper floors and subsequently applied lateral displacements. The FE models were subjected to monotonically increasing instead of cyclic lateral displacement at the top horizontal confining element.

Results of FE Analysis

The incremental horizontal load was applied using Riks algorithm of numerical solution for non-linear systems. Both the models being symmetric load response and other parameters were checked for loading in one direction. The solution could not be carried out upto an ultimate load

or until the failure. Slow convergence in a particular loading increment prematurely terminated the analyses due to a severe cracking and non-linear activities in the model.

Figure 9 shows vector plot of the major principal stress in the masonry portion of the models, which show a prominent formation of diagonal strut in all the models. The struts had a variable width at different portion of the panels and were narrowest at the corners where load was applied and the corner diagonally opposite to those corners. In specimen 2, with more grid elements a larger portion of masonry is stressed to higher degree, representing a more effective utilization of wall material in resisting loads.

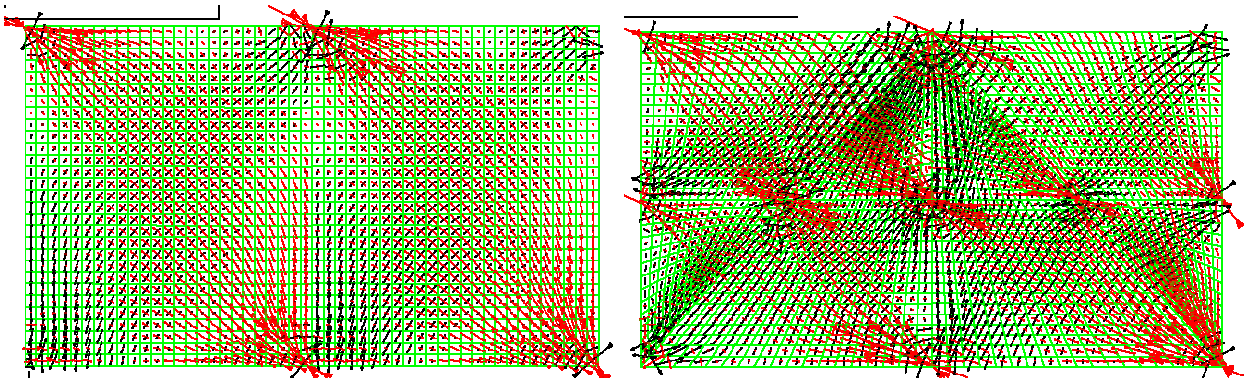

Figure 9 Vector plot of major principal stress in (a) specimen 1 and (b) specimen 2

The ABAQUS load-deformation results for the monotonically increasing loading are compared with the corresponding envelope values measured in the cyclic testing of these specimens in Figure 10. For specimen 1, a close match is seen upto which the analytical result could be obtained before the major cracking appeared in the specimen and the load deformation behaviour was governed by the opening and closing of cracks. For specimen 2, analytical results were stiffer than the experimental results. It seems that analytical model could not adequately capture the sliding of masonry at boundaries with grid elements. Though the analytical model approach had taken into account the sliding in-between masonry and confining grid elements, it could not follow the sliding of bricks through brick joints.

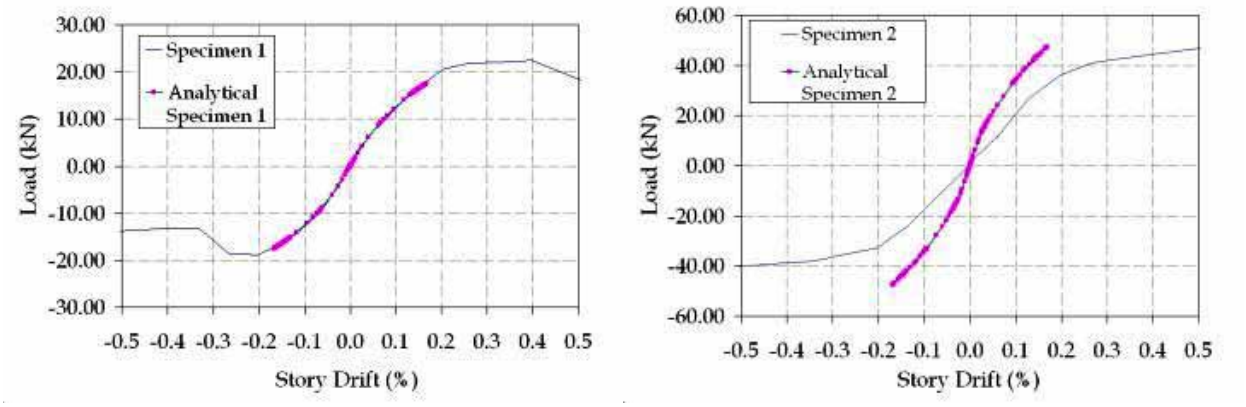

(a) (b)

Figure 10 Comparison between Experimental and FE values of lateral shear for (a) specimen 1

and (b) specimen 2

Conclusions

This study is mainly concerned with improved in-plane lateral resistance of URM walls by the use of confining grid elements. Experimental investigations clearly indicate breaking wall in smaller panels with the use of grid elements can enhance deformability and energy dissipation capacity of such walls. Their placement and spacing greatly influence the behaviour of the system as a whole. As observed, grid elements provide guided shearing plane for sliding of masonry panels under lateral loads, thereby increasing the energy dissipation potential of the confinement scheme. Introduction of diagonal plane of sliding improved the lateral behaviour of confined masonry by sliding along that plane without significant increase of stiffness. A close match is seen between the observed experimental results and estimated analytical results before the major cracking appeared in the specimen and the load deformation behaviour was governed by the opening and closing of cracks. The smeared crack approach is most suitable for predicting the behaviour of masonry when its failure mode is diagonal shear-cracking and results in somewhat poorer prediction when the load deformation is dominated by sliding along bed joints as observed in Specimen 2 even at low displacement levels.

Acknowledgments

The authors are most grateful to the staff of Structural Engineering laboratory at IIT Kanpur for their support and help in the fabrication of specimens and testing. The Ministry of Human Resource Development (MHRD) of Govt. of India, New Delhi, provided funds for this research at IIT Kanpur (Grant No.MHRD/CE/20030315), which is gratefully acknowledged.

References

Bull, J.W. (2001). "Computational Modelling of Masonry, Brickwork and Blockwork Structures," Saxe-Coburg Publications, Dun Eaglasis, Station Brae, Kippen, Stirling, FK8 3DY, UK.

Buonopane, S. G., White, R. N. (1999). "Pseudodynamic Testing of Masonry Infilled Reinforced Concrete Frame," *J. Struct. Engrg.,* ASCE, 125(6), 578-589.

Chuang, S., Zhuge, Y., and McBean, P.C. (2004). "Seismic Retrofitting of Unreinforced Masonry Walls by Cable System," *Proc., 13th World Conf. on Earthquake Engineering*, Vancouver, B. C., Canada, Aug 1-6, 2004, Paper No. 3228.

Gülkan, P., Langenbach, R. (2004) "The Earthquake Resistance of Traditional Timber and Masonry Dwellings in Turkey," *Proc., 13th World Conf. on Earthquake Engineering*, Vancouver, B. C., Canada, Aug 1-6, 2004, Paper No. 2297.

Langenbach, R. (2003) "Survivors amongst the rubble: Traditional Timber-laced Masonry Buildings that Survived the Great 1999 Earthquakes in Turkey and the 2001 Earthquake in India, while Modern Buildings Fell," *Proc., 1st Intnl Congress on Construction History, Instituto Juande Herra, Escuela Técnica Superior de Arquitectura,* Madrid, Vol. 2, 2003: 1257-1268.

Magenes, G., Calvi, G. M. (2002). "In-plane seismic response of brick masonry walls," *J. Earthquake Engineering and Structural Dynamics,* John Wiley & Sons. Ltd., 26, 1091-1112.

Meli, Roberto, Alcocer, S. M. (2004). "Implementation of Structural Earthquake-Disaster Mitigation Programs in Developing Countries," *Natural Hazards Review*, ASCE, 5(1), 29-39.

Paikara, S. (2005). "In-Plane Lateral Resistance of Masonry Confined by Grid Elements," *M.Tech. Dissertation,* Dept. Civ. Engg, Indian Institute of Technology, Kanpur, India.

Rai, D. C. & Goel, S. C. (1996). “Seismic strengthening of unreinforced masonry piers with steel elements.” *Earthquake Spectra*, EERI, vol. 12, no. 4, November, 845-862.